Stable fractional flux vortices and unconventional magnetic state in two-component superconductors

M. A. Silaev

Institute for Physics of Microstructures Russian Academy of Science, 603950 Nizhny Novgorod, Russia and Department of Theoretical Physics, The Royal Institute of Technology, Stockholm, SE-10691 Sweden

(Received 6 August 2010; revised manuscript received 9 November 2010; published 22 April 2011)

In the framework of London theory we study the unconventional magnetic state in two-component superconductors with a finite density of fractional flux vortices stabilized near the surface. We show that the process of vortex entry into the two-component superconductor consists of several steps, while the external magnetic field increases from zero. At the first stage only vortices in one of the order parameter components penetrate and sit at the equilibrium position near the surface. When the magnetic field is increased further, vortices in the second-order parameter component eventually enter the superconductor. Such a complex partial vortex penetration leads to the modification of a Bean-Livingston barrier and a magnetization curve as compared to conventional single-component superconductors. We discuss the possibility of experimental identification of protonic superconductivity in the projected superconducting state of liquid metallic hydrogen and hydrogen-rich alloys with the help of the partial vortex penetration effect.

DOI: 10.1103/PhysRevB.83.144519 PACS number(s): 74.25.Ha, 74.25.Op

I. INTRODUCTION

Recently there has been considerable interest in the physics of superconductors with multiple-order parameter components, which was renewed by the discovery of a number of two-band superconducting materials, such as MgB_2,[1] ferropnictides,[2] heavy fermion compounds,[3] and borocarbides,[4] and advances in experimental techniques[5] providing an intriguing possibility of observing new macroscopic quantum phenomena in liquid metallic hydrogen at ultrahigh pressures.[6–8] Historically the first realization of a two-component superconducting state was considered by Moskalenko[9] and by Suhl, Matthias, and Walker[10] in a metal with two overlapping energy bands on the Fermi surface.

Multiple-component superconductors feature qualitatively new effects, with respect to the conventional ones.[11] One of the striking differences is an unconventional structure of the mixed state in such superconductors. For example, in Ref. 12 it was demonstrated that in a two-band superconductor the interaction between vortices of equal vorticity is not necessarily purely repulsive, but in some cases may be characterized by long-range attraction and short-range repulsion. This in particular leads to the clusterization of vortices and the formation of the "semi-Meissner state," which was recently claimed to be experimentally observed in MgB_2.[13]

Also a rich variety of peculiar vortex states in two-component superconductors have been investigated recently in the framework of the extended Ginzburg-Landau (GL) theory.[14] In particular, there was found a class of solutions of GL equations describing vortices bearing a fractional number of magnetic flux quanta. In general, such vortices can be characterized by different winding numbers of the order parameter in the two superconducting components, i.e., $L_1 \neq L_2$. Among such vortices one can distinguish a subclass of vortices which have $L_1 \neq 0$ and $L_2 = 0$, when the phase winding exists only in one of the condensates. In the present paper we will focus on the simplest case, when $L_1 = \pm 1$ and $L_2 = 0$ (or equivalently $L_2 = \pm 1$ and $L_1 = 0$), further using the term "fractional vortices" to identify such objects. Being positioned at the same point, the two fractional vortices in different condensates characterized by an equal vorticity form a composite vortex bearing a single quantum of magnetic flux.

The fractional vortices in two-component superconductors are qualitatively different from thermodynamically stable exotic topological defects that occur in superfluid and superconducting systems with multiple-order parameter components, such as superfluid ^{3}He (see the review in Ref. 15), ultracold atoms,[16] or vortices in *d*-wave high-temperature superconductivity (HTSC) cuprates with an induced *s*-wave-order parameter component inside the vortex core.[17] The fractional vortices considered in the present work are thermodynamically unstable in bulk two-component superconductors[14] since their energy per unit length is logarithmically or linearly divergent with the sample size. Therefore it is impossible to create the fractional vortices in a bulk superconductor by applying the external magnetic field. This is the reason why up to now fractional vortices in two-component superconductors have not been observed. However, it was proposed that the deconfinement of fractional vortices forming a composite vortex can occur due to thermal fluctuations[18,19] or due to the thermal creation of fractional vortex-antivortex pairs.[20] Also, with the help of GL calculations, fractional vortices were demonstrated to exist in mesoscopic two-component superconductors.[21,22] In the present paper we propose that fractional vortices can be thermodynamically stable near the surface of a superconductor and therefore there is the possibility of creating a finite density of the vortices by an external magnetic field. The finite density of fractional vortices near the surface forms a unconventional magnetic state of the superconductor that should be manifested by a modification of the magnetization curve.

Further, we provide an analytical treatment of London equations describing the behavior of the vortices near the surface of a two-component superconductor. We consider the two-component superconductor as a mixture of two individually conserved superconducting condensates. This model is relevant for the systems where the interband coupling is forbidden by symmetry. Among such systems currently generating great interest is the liquid metallic hydrogen at ultrahigh pressures.[5] In this case two superconducting components were

predicted to originate from electronic and protonic Cooper pairing in metallic hydrogen and hydrogen-rich alloys.[6–8] Since the Cooper pairs of electrons cannot be converted into the Cooper pairs of protons, the interband Josephson interaction is strictly zero. An analogous model of two individually conserved condensates was considered recently in order to describe the exotic states of matter at neutron star inner cores with several charged barionic components, namely, Σ^- hyperons and protons. The mixture of superfluid Σ^- hyperons and protons is analogous to the two-gap superconductor with a strictly zero interband Josephson coupling.[23,24]

On the other hand, in two-band superconductors where the Cooper pairing of electrons takes place in different bands,[9,10] the superconducting condensates in general cannot be considered as individually conserved. However, the model with negligible interband Josephson coupling can be applied also to describe multiband superconductors provided that all relevant physical scales are much shorter than the Josephson length. Although basically considering the system without the interband Josephson coupling, we will discuss on a qualitative level the modification of our results due to this effect.

It is well known that the entry of vortices into a type-II superconductor is hindered by the so-called Bean-Livingston surface barrier.[25,26] This barrier arises due to the competition between two forces acting on the vortex line: a force coming from the Meissner current driving the vortex into the superconductor and a force of the vortex mirror image attracting it toward the outside. As a result, the penetration field H_s of the first vortex entry is typically much larger than the lower critical field H_{c1} and becomes of the order of the thermodynamic critical field H_c.[26] Recently it was demonstrated that a distribution of the Meissner current and the value of the penetration field H_s are highly sensitive to the presence of the Andreev bound state at the surface of d-wave superconductors.[27] It is the goal of the present paper to show that the two-component structure of the order parameter can also alter significantly the value of the penetration field H_s and the process of the vortex entry in two-gap superconductors.

In two-component superconducting systems it is natural to expect that the penetration of fractional vortices in the component with lower condensation energy should occur at a magnetic field which is smaller than H_c. However, since the existence of fractional vortices is prohibited in the bulk, they should sit at a certain distance from the surface, corresponding to the energy minimum. A further increase in the magnetic field will lead to the nucleation of vortices in the second superconducting component. At a final stage of the process of vortex entry, the fractional vortices of different types merge and proliferate into the bulk.

This paper is organized as follows. In Sec. II we give an overview of the theoretical framework, namely, the London theory of two-component superconductors. In Sec. III we discuss the Gibbs energy of fractional vortices near the surface and address the questions of fractional vortex stability and the Bean-Livingston barrier for penetration of fractional vortices. Also we calculate the equilibrium distribution of fractional vortices near the surface. In Sec. IV we discuss the modification of the magnetization curve due to the partial vortex penetration, and the possibility to implement the experimental identification of two-order parameter components in the projected superconducting state of liquid metallic hydrogen. We give our conclusions in Sec. V.

II. BASIC EQUATIONS: LONDON THEORY OF FRACTIONAL VORTICES IN A TWO-GAP SUPERCONDUCTOR

Let us consider a superconductor with two coexisting superconducting condensates. The external magnetic field is directed along the z axis, $\mathbf{H_0} = H_0\mathbf{z_0}$. Considering the London limit, i.e., assuming that the coherence length is vanishingly small compared to all other length scales, we obtain the Gibbs energy per unit length along the z axis as follows:[19]

$$F_G = F - \frac{1}{4\pi}\int \mathbf{H}\cdot\mathbf{H}_0\, d^2r, \tag{1}$$

where the free energy is

$$F = \frac{1}{8\pi}\int\left[\mathbf{H}^2 + \lambda_A^{-2}\left(\mathbf{A} - \frac{\phi_0}{2\pi}\nabla\theta_A\right)^2 + \lambda_B^{-2}\left(\mathbf{A} - \frac{\phi_0}{2\pi}\nabla\theta_B\right)^2\right] d^2r. \tag{2}$$

Here $\lambda_{A,B}$ are the different length scales, proportional to the densities of two types of superconducting carriers, $\mathbf{H}$ is a total magnetic field, $\mathbf{A}$ is a vector potential, and $\theta_{A,B}$ are the phases of superconducting order parameters. As we will see further, the London limit in the two-component model that we consider yields an exponential decaying magnetic field generated by fractional vortices. On the other hand, it was recently demonstrated that in a full two-component GL theory there is always a power-law tail of magnetic field around a fractional vortex.[28] However, the power-law behavior of the magnetic field starts at the distances greater than the London penetration depth λ, which is considered to be the largest length scale in our present paper. For example, as we will see below, the intervortex distance in the proposed unique magnetic state of the two-component superconductor is much smaller than λ. Within this parameter range. the London model is a good approximation to study the magnetic properties of two-component superconductors.

The London-Maxwell (LM) equation for the magnetic field obtained from the condition $\delta F/\delta\mathbf{A} = 0$ yields

$$\lambda^2\nabla\times\mathbf{H} = -\mathbf{A} + \frac{\phi_A}{2\pi}\nabla\theta_A + \frac{\phi_B}{2\pi}\nabla\theta_B, \tag{3}$$

where $\lambda^2 = \lambda_A^2\lambda_B^2/(\lambda_A^2+\lambda_B^2)$ is the London penetration depth, and $\phi_{A,B} = \phi_0(\lambda/\lambda_{A,B})^2$ are partial magnetic fluxes so that $\phi_A + \phi_B = \phi_0$. With the help of LM equation (3), the free energy (1) can be rewritten as a superposition of two parts,

$$F = F_m + F_{nc}, \tag{4}$$

where the first part is the sum of total magnetic energy and the kinetic energy of the superconducting current and thus depends only on the magnetic field,

$$F_m = \frac{1}{8\pi}\int[\mathbf{H}^2 + \lambda^2(\nabla\times\mathbf{H})^2]d^2r. \tag{5}$$

The second part F_{nc} is the kinetic energy of relative motion of two condensates, which can be associated with the

neutral superfluid current, supported by the counterdirected motion of equally charged particles (electrons in two-gap superconductors) or codirected motion of oppositely charged ones (electrons and protons in superconducting liquid metallic hydrogen).[11] This term depends on the relative phase difference between two condensates $\varphi_{\rm rel} = \theta_A - \theta_B$ as follows:

$$F_{nc} = \frac{1}{2\pi}\frac{\phi_A\phi_B}{(4\pi\lambda)^2}\int(\nabla\varphi_{\rm rel})^2 d^2r. \tag{6}$$

Such a division of the total energy (4) is convenient for the calculations since the parts F_m and F_{nc} can be found independently.

For example, the energy F_m of one fractional vortex in an A or B condensate can be calculated exactly in a same scheme as for the case of a conventional single-gap superconductor.[26] The result is

$$F_m = \varepsilon_i + \frac{\phi_i}{8\pi}H_v(\mathbf{R_i}), \tag{7}$$

where $i = A, B$ and $\mathbf{R_i}$ is the fractional vortex coordinate. The first term in Eq. (7) is the is the self-energy of the vortex,

$$\varepsilon_i = \left(\frac{\phi_i}{4\pi\lambda}\right)^2 \ln(\lambda/\xi_i),$$

where ξ_i is the coherence length, and the second term in Eq. (7) is the energy in the magnetic field $\mathbf{H_v} = H_v\mathbf{z_0}$ generated by other vortices.

In an infinite superconducting sample the part of energy F_{nc} given by (6) is divergent for a single fractional vortex due to the unscreened currents induced in the vortex-free phase.[14] Indeed, taking, for example, $\theta_A = \arctan(y/x)$ and $\theta_B = 0$, we get that $(\nabla\varphi_{\rm rel})^2 \sim 1/r^2$, which means that expression (6) is logarithmically divergent with the size of the superconducting sample L so that $F_{nc} \sim \ln L$. However, further on we will see that in some specific cases the energy of a single fractional vortex can be finite. In particular, such a situation is realized for a fractional vortex placed near the boundary of the superconductor. In this case the large-scale divergence in Eq. (6) is removed due to the cancellation of the unscreened superconducting current in the vortex-free phase due to the image antivortex.

III. RESULTS

A. Gibbs energy of fractional vortices near the surface of the superconductor

A sketch of the system considered is shown in Fig. 1. It consists of a two-component superconductor, occupying the half space $x > 0$ bounded by the yz plane. Our goal is to calculate the Gibbs energy (1) of the vortex configuration shown in Fig. 1, i.e., of the two vortices in the A and B phases located at the points $\mathbf{R_A} = (x_A,0)$ and $\mathbf{R_B} = (x_B,0)$ near the surface. Here we can consider only vortices positioned in a line since any relative shift of A and B vortices along the boundary plane leads to increasing energy.

All vortices are directed along the z axis, which is parallel to the boundary plane. Since neither Meissner currents nor vortices parallel to the surface create magnetic fields outside the superconductor,[26] the integration in Eq. (1) can be restricted to the superconducting region only. Furthermore, in Eq. (2)

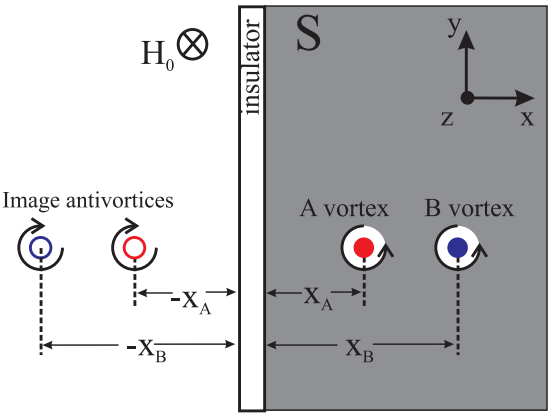

FIG. 1. (Color online) The sketch of the system under consideration. It consists of a two-component superconductor occupying the half space $x > 0$ bounded by the yz plane. The fractional vortices are situated at distances x_A and x_B from the boundary. The boundary conditions are taken into account by placing image antivortices at the proper points behind the boundary plane.

we can take into account only the magnetic field generated by the vortices and neglect the field generated by the Meissner current. Then to calculate the energy we should find the magnetic field $\mathbf{H}(\mathbf{r})$ generated by the vortices and the relative phase distribution $\varphi_{\rm rel}(\mathbf{r})$.

The magnetic field is determined by the LM equation having the following form:

$$\lambda^2\nabla\times\nabla\times\mathbf{H} + \mathbf{H} = \mathbf{z_0}[\phi_A\delta(\mathbf{r}-\mathbf{R_A}) + \phi_B\delta(\mathbf{r}-\mathbf{R_B})]. \tag{8}$$

Varying expression (6) with respect to the phase difference $\varphi_{\rm rel}$, we obtain the following two-dimensional (2D) Poisson equation with the sources at the points of the vortex positions:

$$\Delta\varphi_{\rm rel} = 2\pi[\delta(\mathbf{r}-\mathbf{R_A}) - \delta(\mathbf{r}-\mathbf{R_B})]. \tag{9}$$

Equations (8) and (9) should be supplemented by the boundary conditions at the surface of the superconductor,

$$\mathbf{x_0}\cdot\left(\mathbf{A} - \frac{\phi_0}{2\pi}\nabla\theta_{A,B}\right)|_{x=0} = 0, \tag{10}$$

which means vanishing of the superconducting current through the boundary in both of the condensates. These boundary problems can be treated by using the method of images, i.e., by placing the image antivortices in the A and B phases at the points $\tilde{\mathbf{R}}_{\mathbf{A,B}} = (-x_{A,B},0)$, respectively (see Fig. 1). Then, the free energy of the two-vortex molecule near the flat surface of the superconductor is just one half of the free energy of the vortex-antivortex molecule (Fig. 1).

Let us evaluate the energy F_m given by expression (5). For the stack of several vortices it is given by the sum of the individual vortex energies (7). The magnetic field $\mathbf{H} = H_v\mathbf{z_0}$ generated by the vortex currents can be taken by the superposition of fields produced by vortices at points $\mathbf{R_{A,B}}$ and antivortices at points $\tilde{\mathbf{R}}_{\mathbf{A,B}}$:

$$H_v = H_{v1} + H_{v2} + H_{av1} + H_{av2},$$

where

$$H_{v1} = \frac{\phi_A}{2\pi\lambda^2} K_0\left(\frac{|\mathbf{r}-\mathbf{R_A}|}{\lambda}\right),$$
$$H_{v2} = \frac{\phi_B}{2\pi\lambda^2} K_0\left(\frac{|\mathbf{r}-\mathbf{R_B}|}{\lambda}\right),$$
$$H_{av1} = -\frac{\phi_A}{2\pi\lambda^2} K_0\left(\frac{|\mathbf{r}-\tilde{\mathbf{R}}_\mathbf{A}|}{\lambda}\right),$$
$$H_{av2} = -\frac{\phi_B}{2\pi\lambda^2} K_0\left(\frac{|\mathbf{r}-\tilde{\mathbf{R}}_\mathbf{B}|}{\lambda}\right),$$

where $K_0(x)$ is the zero-order Hankel function, having the asymptotic $K_0(x) \approx C - \ln(x)$ at $x \ll 1$ and $K_0(x) \approx \sqrt{\pi/2x}e^{-x}$ at $x \gg 1$.[29] Thus for the energy F_m we obtain

$$F_m = \varepsilon_A + \varepsilon_B + \frac{\phi_A\phi_B}{(4\pi\lambda)^2}\left[2K_0\left(\frac{|x_A - x_B|}{\lambda}\right) - 2K_0\left(\frac{|x_A + x_B|}{\lambda}\right) - \sigma K_0\left(\frac{2x_A}{\lambda}\right) - \frac{1}{\sigma}K_0\left(\frac{2x_B}{\lambda}\right)\right], \tag{11}$$

where we introduce the coefficient $\sigma = \phi_A/\phi_B$.

To calculate the other part of free energy F_{nc} we should substitute into Eq. (6) the relative phase distribution in the form, corresponding to the case when the A and B vortices are situated at the points $\mathbf{R_A} = (x_A,0)$ and $\mathbf{R_B} = (x_B,0)$ and image A and B antivortices are situated at the points $\tilde{\mathbf{R}}_\mathbf{A} = (-x_A,0)$ and $\tilde{\mathbf{R}}_\mathbf{B} = (-x_B,0)$ correspondingly:

$$\nabla\varphi_{\rm rel} = \frac{\mathbf{r}-\mathbf{R_A}}{|\mathbf{r}-\mathbf{R_A}|^2} - \frac{\mathbf{r}-\tilde{\mathbf{R}}_\mathbf{A}}{|\mathbf{r}-\tilde{\mathbf{R}}_\mathbf{A}|^2} - \frac{\mathbf{r}-\mathbf{R_B}}{|\mathbf{r}-\mathbf{R_B}|^2} + \frac{\mathbf{r}-\tilde{\mathbf{R}}_\mathbf{B}}{|\mathbf{r}-\tilde{\mathbf{R}}_\mathbf{B}|^2}. \tag{12}$$

The result is

$$F_{nc} = \frac{\phi_A\phi_B}{(4\pi\lambda)^2}\left[\ln\left(\frac{2x_A}{\xi_A}\right) + \ln\left(\frac{2x_B}{\xi_B}\right) - 2\ln\left|\frac{x_A + x_B}{x_A - x_B}\right|\right]. \tag{13}$$

Note that expression (11) for the energy F_m as well as expression (13) for F_{nc} are valid only when the separations between vortices are larger than the coherence lengths: $x_A > \xi_A$, $x_B > \xi_B$, and $|x_A - x_B| > \max(\xi_A,\xi_B)$. However, the last restriction is removed when the total free energy

$$F_{vv}(x_A,x_B) = F_m(x_A,x_B) + F_{nc}(x_A,x_B)$$

is considered. Indeed, in this case the logarithmic singularities at $x_A = x_B$ in Eqs. (11) and (13) cancel each other. Therefore the expression for the total free energy $F_{vv}(x_A,x_B)$ given by the sum of partial energies (11) and (13) can be used for any values of the vortex coordinates $x_A > \xi_A$ and $x_B > \xi_B$.

Finally let us consider the second term in Eq. (1) which determines the interaction of vortices with the external magnetic field. This interaction energy can be written as

$$W = -\frac{H_0\Phi}{4\pi}, \tag{14}$$

where $\Phi = \int H_v\, d^2\mathbf{r}$ is the total magnetic flux generated by the vortex currents. Due to the linearity of the LM equation (8) and the boundary condition (10) the magnetic flux can be decomposed into the contributions from A and B vortices:

$$\Phi = \Phi_A + \Phi_B.$$

In accordance with the consideration of Ref. 26, these partial magnetic fluxes depend on the positions of fractional vortices in the following way:

$$\Phi_A = \phi_A(1 - e^{-x_A/\lambda}), \tag{15}$$

$$\Phi_B = \phi_B(1 - e^{-x_B/\lambda}). \tag{16}$$

Thus for the energy of vortex interaction with the external magnetic field we finally obtain

$$W(x_A,x_B) = -\frac{H_0}{4\pi}[\phi_A(1 - e^{-x_A/\lambda}) + \phi_B(1 - e^{-x_B/\lambda})]. \tag{17}$$

B. Stable fractional vortices

Summing up the different parts of the free energy (11) and (13) and the energy of interaction with the external magnetic field (17) we obtain the Gibbs energy

$$F_G(x_A,x_B) = F_{vv}(x_A,x_B) + W(x_A,x_B). \tag{18}$$

The equilibrium vortex positions are determined by the extremum of the Gibbs energy, which is given by the condition

$$\frac{\partial F_G}{\partial x_A}(x_A^*,x_B^*) = 0, \qquad \frac{\partial F_G}{\partial x_B}(x_A^*,x_B^*) = 0, \tag{19}$$

if both $x_A^* > \xi_A$, $x_B^* > \xi_B$, or otherwise by the condition

$$\frac{\partial F_G}{\partial x_A}(x_A^*,\xi_B) = 0, \qquad \frac{\partial F_G}{\partial x_B}(\xi_A,x_B^*) = 0, \tag{20}$$

when only one fractional vortex enters the superconductor.

As is shown in left-hand panel of Fig. 2, for a sufficiently large magnetic field there can be realized a situation when the fractional vortices are stable near the surface. In general it corresponds to the extremum condition (20), which means that the fractional vortices of different types cannot coexist, i.e., either $x_B^* = 0$ and $x_A^* \neq 0$ or $x_A^* = 0$ and $x_B^* \neq 0$. Another alternative is given by condition (19), which is satisfied only for a composite vortex with $x_B^* = x_A^* \neq 0$, but it is impossible to realize a regime of stable molecules of fractional vortices near the surface with $x_B^* \neq x_A^* \neq 0$.

Let us now discuss in more detail the dependence of the equilibrium position of a fractional vortex on the external magnetic field $\mathbf{H_0} = H_0\mathbf{z_0}$. To be definite we consider the case of the A phase vortex. Then the equation which determines x_A^* follows from condition (20) and has the following form:

$$\left[K_1(y) + \frac{1}{\sigma y}\right]e^{y/2} = 2\pi\frac{H_0}{H_\lambda^A}, \tag{21}$$

where $y = 2x_A^*/\lambda$ and $H_\lambda^A = \phi_A/(2\pi\lambda^2)$. The solution of this equation is plotted in the right-hand panel of Fig. 2 as a

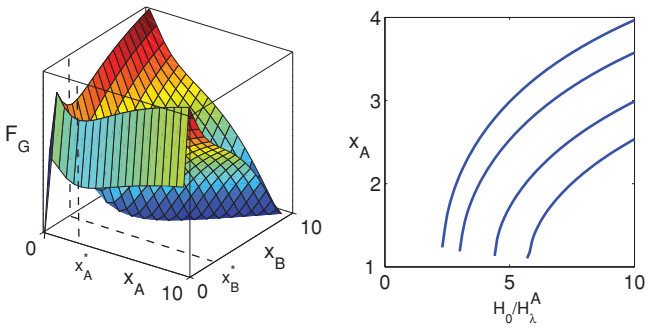

FIG. 2. (Color online) Left-hand panel: Gibbs energy of the molecule consisting of two fractional vortices near the surface of the superconductor. The parameters are $\xi_A = \xi_B$ and $\phi_A = \phi_B$. The magnetic field is taken to be $H_0 = 5H_\lambda$. In this plot the local energy minima are clearly seen at $x_B = 0$, $x_A = x_A^*$ and $x_A = 0$, $x_B = x_B^*$. Right-hand panel: The dependence of the fractional vortex position x_A^* on the magnetic field H_0 for different values of $\phi_A/\phi_B = 1,2,3,4$ (from top to bottom curve). All lengths are normalized to the scale λ.

function of external magnetic field H_0 for different values of the coefficient $\sigma = 1,2,3,4$ (from top to bottom curve). Several qualitative features which characterize the behavior of fractional vortices near the surface can be deduced from Fig. 2(b). First, the distance x_A^* is scaled in the penetration depth λ. This length scale is determined by the decay length of the interaction of vortex with the external field, i.e., the energy $W(x_A)$. Second, the vortex coordinate x_A^* grows monotonically with the external field H_0. Such behavior is explained by the fact that the force pushing the vortex toward the bulk of the superconductor is proportional to H_0. Thus the larger is the pushing force, the further can the fractional vortex penetrate into the superconductor. Finally, the minimal magnetic field which provides the local Gibbs energy minimum for $x_A^* \neq 0$ is of the order of $H_\lambda^A = \phi_A/(2\pi\lambda^2)$.

As we have shown above, if the external magnetic field is larger than the threshold value of the order of $H_\lambda^i = \phi_i/(2\pi\lambda^2)$, where $i = A,B$, there appears a minimum of the fractional vortex energy which determines the equilibrium vortex position $x_i^* > 0$. The Gibbs energy minima occur both for the A and B vortices for an arbitrary ratio of the fractional fluxes ϕ_A and ϕ_B as well as of the coherence lengths ξ_A and ξ_B. For example, in the left-hand panel of Fig. 2, the energy minima are shown to exist at $x_A^* \neq 0$, $x_B^* = 0$, and $x_B^* \neq 0$, $x_A^* = 0$ for a two-gap superconductor with $\phi_A = \phi_B$ and $\xi_A = \xi_B$.

Thus we can conclude that fractional vortices can be stable near the surface of a superconductor for arbitrary values of parameters ϕ_A,ξ_A and ϕ_B,ξ_B characterizing the two superconducting condensates. Still the consideration above is not complete because it misses a very important question of how the fractional vortices can be created in the superconducting region. In the next section we will see that the scenario of vortex penetration is sensitive to the ratio of the coherence lengths ξ_A and ξ_B of two different condensates.

C. Bean-Livingston barrier and the critical field of the first vortex entry

To begin with the analysis of vortex penetration, we note first that the condition for Bean-Livingston barrier suppression derived in Ref. 26 should be modified here to take into account the peculiarities of a two-gap superconductor case. This condition takes the following form:

$$(\mathbf{n}\cdot\nabla F_G)(x_A = \xi_A, x_B = \xi_B) < 0 \tag{22}$$

for some vector $\mathbf{n} = (n_A,n_B)$ satisfying the condition $n_A > 0$, $n_B > 0$. With the help of the expression for the Gibbs energy given by Eqs. (11), (13), (17), and (18), it is possible to obtain an analytical expression for the critical value of magnetic field $H_0 = H_s$ suppressing the surface barrier.

It occurs that the two different regimes of vortex entry are determined by the ratio of coherence lengths of two superconducting components ξ_A and ξ_B.

(i) The case when $\xi_A = \xi_B = \xi$ always corresponds to the simultaneous entrance of two fractional vortices. As one can see in Fig. 3(a), the surface barriers for two vortices disappear at the same value of the critical field $H_0 = H_s$, which is estimated as

$$H_s = \frac{\phi_0}{4\pi\lambda\xi}. \tag{23}$$

(ii) The case when $\xi_A \neq \xi_B$ is more interesting. Indeed, in Fig. 3(b) it is clearly shown that there is a range of magnetic fields when for one of the superconducting condensates the Bean-Livingston barrier is already suppressed while for the other it still exists. The critical field of the first vortex entry $H_0 = H_{s1}$ is given by

$$H_{s1} = \min(H_{sA}, H_{sB}), \tag{24}$$

where $H_{sA} = \phi_0/(4\pi\lambda\xi_A)$ and $H_{sB} = \phi_0/(4\pi\lambda\xi_B)$. Therefore, the vortex with a larger core size $\xi_A > \xi_B$ is the first one to penetrate the superconductor.

Thus we conclude that in some range of parameters it is possible that vortices penetrate by parts, i.e., only the fractional vortices in one of the condensates appear at first in the superconductor. Such a situation is possible when the coherence lengths of the two condensates are different, $\xi_A \neq \xi_B$. In this case the vortex penetration occurs according to the following scenario. If the external magnetic H_0 field

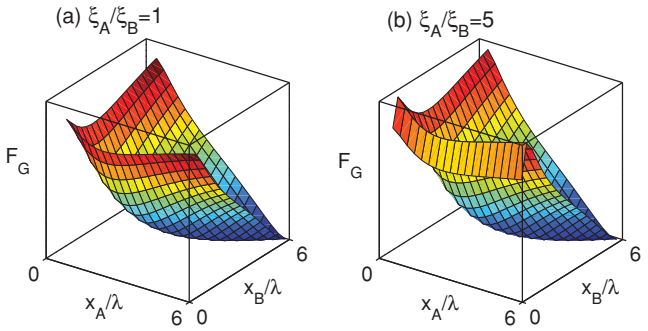

FIG. 3. (Color online) Gibbs energy of the molecule consisting of two fractional vortices near the surface of the superconductor. (a) Equal coherence lengths of two condensates $\xi_A/\xi_B = 1$. In this case the Bean-Livingston barrier is suppressed simultaneously for fractional vortices of both types. (b) Different coherence lengths of two condensates $\xi_A/\xi_B = 5$. In this case the barrier is suppressed for the fractional vortex in the A condensate while for the B condensate it still exists.

is increased from zero, then at the threshold value $H_0 = H_{s1}$ the Bean-Livingston barrier is suppressed and the fractional vortices with a larger core size enter the superconductor. However, they cannot proliferate into the bulk and sit at some equilibrium position near the surface of the superconductor. The equilibrium position of one fractional vortex is determined by Eq. (21) and its dependence on the external field is shown in the right-hand panel of Fig. 2. When the magnetic field H_0 is increased further and reaches the second threshold field $H_0 = H_{s2}$, determined by

$$H_{s2} = \max(H_{sA}, H_{sB}), \tag{25}$$

then the surface barrier is suppressed for the vortices in the second condensate. As one can see from Fig. 3 the fractional vortices in A and B condensates always merge to form a composite vortex and proliferate into the bulk superconductor since the total minimum of the Gibbs energy is always reached at $x_A^* = x_B^*$. Therefore, we can conclude that if $\xi_A \neq \xi_B$, then at the range of magnetic fields $H_{s1} < H_0 < H_{s2}$ the fractional vortices should appear near the surface of a two-gap superconductor.

Note that above we have analyzed only the single-vortex problem. However, it is natural to expect that when the Bean-Livingston barrier for fractional vortices is suppressed, they penetrate into the superconductor until some equilibrium vortex distribution is set up near the surface. Below we will find the equilibrium distribution of fractional vortices at the range of magnetic fields $H_{s1} < H_0 < H_{s2}$.

D. Unconventional magnetic state with finite density of fractional vortices near the surface

Now we consider the unconventional magnetic state of a two-component superconductor which is realized when the finite density of stable fractional flux vortices appears near the surface as the magnetic field exceeds the critical field of the first vortex entry H_{s1}. To be definite we assume that $\xi_A > \xi_B$, and therefore the vortex in the A phase is the first one to enter the superconductor since $H_{sA} < H_{sB}$.

In general, the task of finding the equilibrium configuration of fractional vortices stabilized near the surface of the superconductor seems to be rather complicated. One of the reasons is a many-body origin of this problem, resulting in a huge number of dimensions of a configuration space. However, here we can use a simplified approach which is based on the consideration of a distribution of an average density of fractional vortices. Such treatment is justified by the fact that in a magnetic field of the order H_{sA} the intervortex distance is of the order of $a \sim \sqrt{\lambda\xi_A}$. As we have shown above, the fractional vortices sit at a distance $d \sim \lambda$ from the surface, which is much larger than the characteristic intervortex distance.

So we assume that the A phase vortices are distributed in space with a density $n(\mathbf{r})$, where $\mathbf{r} = (x, y)$. To find the form of the equilibrium vortex distribution $n(\mathbf{r})$ we should consider a probe vortex positioned at some point $\mathbf{r_v} = (x_v, y_v)$ and place a requirement of its stationarity, i.e., that the total force acting on the probe vortex is to be zero,

$$f = \frac{\partial}{\partial x_v} F_G(x_v) = 0.$$

The expression for the Gibbs energy consists of three parts, namely,

$$F_G(x_v) = F_m(x_v) + F_{nc}(x_v) + W(x_v),$$

given by Eqs. (5), (6), and (14) correspondingly. So to calculate the force we should determine the dependence of three energy parts on the position of the probe vortex. This leads to the following integral equation for the vortex density $n(x)$ (the details of calculation are given in the Appendix):

$$\alpha \int_0^\infty \left[\frac{(x - x_v)}{|x - x_v|} e^{-|x-x_v|} + e^{-|x+x_v|} \right] n(x) dx + \beta \int_{x_v}^\infty n(x) dx = \gamma e^{-x_v}, \tag{26}$$

where $\alpha = \phi_A^2/(16\pi\lambda)$, $\beta = \phi_A\phi_B/(8\pi\lambda)$, and $\gamma = \phi_A H_0/(8\pi\lambda)$. In Eq. (26) the coordinates x and x_v are normalized to the length scale λ.

The integral Eq. (26) can be solved analytically. Differentiating three times both sides of Eq. (26) over x_v, we obtain the differential equation for $n(x)$:

$$\frac{d^2 n}{dx^2} = \frac{\beta}{\beta + 2\alpha} n. \tag{27}$$

Therefore, the solution $n(x)$ has the form

$$n(x) = A e^{-x/L_n}, \tag{28}$$

where the scale L_n and the amplitude A are determined by Eqs. (26) and (27) as follows (here we restore the length normalization factor λ):

$$L_n = \lambda \sqrt{\frac{2\alpha + \beta}{\beta}} = \lambda \sqrt{1 + \phi_A/\phi_B}, \tag{29}$$

$$A = \frac{\gamma}{\alpha} \frac{\left(L_n^2 - \lambda^2\right)}{2L_n^2} = \frac{H_0}{\phi_A} \frac{\left(L_n^2 - \lambda^2\right)}{L_n^2}. \tag{30}$$

Thus we obtain that the concentration of fractional vortices $n(x)$ given by Eqs. (28)–(30) decays exponentially with the distance from the surface of the superconductor. Note that in the case of ordinary vortices (which is obtained by putting $\beta = 0$ in the expressions above) we get that $L_n = \infty$, which means that the vortex density is constant.[26] The difference in the behavior of ordinary and fractional vortex density $n(x)$ is provided by an additional force which is determined by the gradient of energy $F_{nc}(x)$ (6). This force pushes the fractional vortices out of the superconductor. Qualitatively this force is explained by the fact that the existence of fractional vortices is not allowed in the bulk superconductor due to the infinite energy of such objects.

Let us find a contribution of fractional vortices to the average magnetization of a superconducting sample. To distinguish from the magnetization provided by Meissner currents, we denote this contribution as $\mathbf{M_f} = M_f \mathbf{z_0}$. Then we have

$$M_f = \frac{1}{4\pi L} \int_0^\infty n(x) \Phi_A(x) dx, \tag{31}$$

where $n(x)$ is the vortex density, L is the sample size in the x direction (see Fig. 1) and $\Phi_A(x)$ is the total magnetic flux (15) provided by one fractional vortex placed at a distance

x from the boundary. Substituting expression (28) for the vortex density into Eq. (31), we obtain that

$$M_f = \frac{H_0}{4\pi}\frac{L_n - \lambda}{L}. \tag{32}$$

IV. DISCUSSION

Now, with the help of the results of the previous section, let us consider the properties of the magnetization curve of a two-gap superconductor. The qualitative features of the magnetization should be determined by the following facts.

(i) In increasing magnetic field the vortices penetrate into the superconductor by parts. When the magnetic field reaches the critical value (24), the fractional vortices with a larger core size proliferate into the superconducting region.

(ii) For the range of magnetic fields $H_{s1} < H_0 < H_{s2}$, only fractional vortices of one type exist near the surface of the superconductor. Their distribution is determined by Eqs. (28)–(30). When the magnetic field becomes larger, $H_0 > H_{s2}$, the fractional vortices of the other type penetrate. Then fractional vortices of different types merge and composite vortices proliferate into the bulk superconductor. The value of the field H_{s2} is certainly modified by the presence of a finite density of fractional vortices in the first condensate. The modified value of H_{s2} can be found by calculating the forces acting on a single fractional vortex in the second condensate in a same way as that on the first condensate (see the Appendix). Then we obtain that in this case the critical field is reduced by the factor $\sqrt{\phi_B/\phi_0}$ as compared to Eq. (25), where ϕ_B is a magnetic flux carried by fractional vortices in the second condensate.

Thus we can work out the following qualitative picture of the superconducting sample magnetization behavior with increasing magnetic field. At low fields $H_0 < H_{s1}$, the magnetization is determined by the Meissner current. If all the stray fields are neglected it is given by

$$M_1 = -\frac{H_0}{4\pi}. \tag{33}$$

For magnetic fields in the range $H_{s1} < H_0 < H_{s2}$, the magnetization is changed due to the fractional vortices

$$M_2 = M_f(H_0) - \frac{H_0}{4\pi}, \tag{34}$$

where $M_f(H_0)$ is given by Eq. (32). Finally at $H_0 > H_{s2}$ the magnetization changes abruptly and becomes

$$M_3 = \frac{B(H_0) - H_0}{4\pi}, \tag{35}$$

where the net magnetic induction $B(H_0)$ is determined by the configuration of the vortex lattice in the bulk superconductor (see, for example, Refs. 26 and 30).

These qualitative features of the magnetization curve are summarized in Fig. 4, where the magnetic-field dependence of the average magnetization of the superconducting sample $M(H_0)$ is shown for the case of single-gap (left-hand panel) and two-gap (right-hand panel) superconductors. For a single-gap superconductor we have a conventional picture of the Meissner state overheating due to the Bean-Livingston barrier. In the left-hand panel of Fig. 4 we show the three characteristic

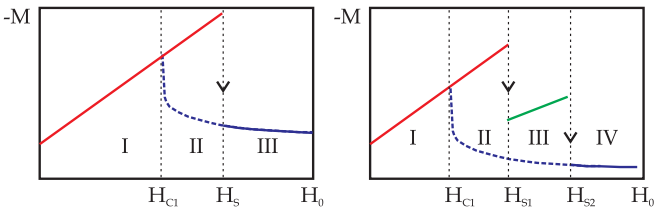

FIG. 4. (Color online) Qualitative behavior of magnetization curve of a superconductor modified due to the surface barrier. Left-hand panel: Single-gap superconductor. Right-hand panel: Two-gap superconductor.

regions corresponding to this case. At region (I), when the magnetic field is smaller than the first critical one H_{c1}, the Meissner state is realized. At region (II), where $H_{c1} < H_0 < H_s$, where $H_s = \phi_0/(4\pi\lambda\xi)$, the Meissner state is overheated due to the Bean-Livingston barrier. Correspondingly, the total magnetization still grows at this region (solid line) instead of following the bulk sample curve (dashed line). Finally at $H_0 = H_s$ the surface barrier is suppressed and the magnetization jumps to the value determined by the configuration of vortices in the bulk of the superconductor.

In contrast to the conventional scheme, a two-gap superconductor features two jumps of the magnetization curve (right-hand panel of Fig. 4). Correspondingly, there are four regions which are characterized by a qualitatively different behavior of the $M(H_0)$ dependence. Regions (I), where $H_0 < H_{c1}$, and (II), where $H_{c1} < H_0 < H_{s1}$, are the same as for a conventional superconductor. A nontrivial behavior starts at the field $H_0 = H_{s1}$ of the first vortex entry. At this threshold field value there is a jump in the magnetization curve, which is determined by a setup of a finite concentration of fractional vortices near the surface of the superconductor. At region (III) for the range of magnetic fields $H_{s1} < H < H_{s2}$ the magnetization is determined by Eqs. (32) and (34) and grows linearly with H_0. The second jump of the $M(H_0)$ curve occurs at the field $H_0 = H_{s2}$ when the composite vortices start to proliferate into the bulk of the superconductor. Finally at region (IV), when $H_0 > H_{s2}$, the value of magnetization is determined by the configuration of composite vortices in the bulk of the superconductor.

The above-discussed possibility of separate vortex penetration in two coexisting superconducting condensates should be especially interesting in connection with the investigation of the projected superconducting state of liquid metallic hydrogen,[6,7] where the superconducting state is formed by electronic and protonic Cooper pairs. The observation of the two-component superconducting state in this case cannot be implemented by conventional techniques and requires special experimental approaches.[8] In particular, the most challenging problem of the protonic superconductivity detection cannot be treated by the standard measurement of the Meissner effect since the critical temperature for electrons is estimated to be much larger than that of protons. Therefore, in the Meissner state the contribution to the total magnetic moment of the protonic supercurrent will be always masked by that of the electronic component. On the other hand, as we have shown above, the relaxation of the overheated Meissner state by vortex penetration should feature an additional jump in

magnetization due to the coexistence of protonic and electronic superconducting components. According to our results, the critical magnetic field of the first vortex entry is determined by the condensate with the largest coherence length, which is the one with the smallest critical temperature. In liquid metallic hydrogen such a component is always a protonic one, therefore the first jump in the magnetization curve should be determined by the vortices in the protonic superfluid, provided it is type II. According to the recent estimations the low-temperature limit of magnetic flux carried by vortices in the protonic component is of the order $\phi_p(T=0) \sim 10^{-3}\phi_0$, which is several orders of magnitude larger than the resolution threshold in modern experiments[8] that allow to detect magnetic fluxes of less than $10^{-5}\phi_0$. Therefore, even for temperatures close to the critical one of the protinic component, it is possible to detect the protonic vortices. It is interesting to note that on approaching the critical temperature of the protonic component from below the field of fractional vortex penetration in the protonic condensate reduces to zero. Therefore the largest interval of magnetic fields where only the fractional vortices should exist near the surface is in the vicinity of the protonic critical temperature.

Finally we note that, besides the intriguing possibility of exploring the nature of the superconducting state in liquid metallic hydrogen, our results are applicable to the case of a conventional two-gap superconductor. Generally speaking, in this case, one should take into account the effect of interband Josephson coupling that we have neglected. This assumption is justified in the case when the Josephson length of the intercomponent phase difference relaxation is much larger than the other relevant length scales, which are the coherence lengths in both condensates and the London penetration length. However, even if this condition is violated, the critical magnetic field of the first vortex entry H_{s1} remains the same, i.e., it is not affected by the presence of the Josephson coupling since the energy of the Josephson string connecting the fractional vortex with the surface grows quadratically at small distances (see, e.g., Ref. 31) and does not alter the condition of vortex penetration (22). The further penetration of the vortex in the second component is certainly affected by the presence of the first fractional vortex emanating from the Josephson string ending at the surface. Presumably, the result should be the reduction of the field H_{s2} of the second vortex entry, however, the strict quantitative investigation of this effect is beyond the scope of the present paper. Thus we can conclude that our main result, i.e., the separate penetration of fractional vortices and the presence of two jumps on the magnetization curve, remains qualitatively relevant even in case of a rather strong intercomponent Josephson interaction.

V. SUMMARY

To summarize, we have investigated the unconventional magnetic state of two-component superconductors. This peculiar state is realized when the finite density of stable fractional vortices appears near the surface of the superconductor under the action of an external magnetic field. This result contrasts to the case of a bulk two-component superconductor where fractional vortices have infinite energy and therefore cannot exist.[14] In our situation the stability of fractional vortices near the surface is provided by the cancellation of the unscreened superconducting current due to the image antivortices.

Also we have discussed the influence of fractional vortices on a Bean-Livingston barrier and the magnetization curve of a two-component superconductor. In particular, we have found that if the coherence lengths of two condensates are different, then vortices penetrate the superconductor by parts. The fractional vortices in the condensate with a larger coherence length, i.e., having a larger core size, are the first to enter the superconductor. By increasing the magnetic field further, the fractional vortices in the second condensate are pushed to penetrate. Then the fractional vortices of two different types merge to form composite vortices which proliferate into the bulk superconductor.

We have shown that the magnetization curve of a superconduting sample should feature the two jumps associated with the penetration of two types of fractional vortices. The observation of such a peculiar magnetization behavior could be considered as an experimental identification of fractional vortices in systems with several superconducting components, such as multiband superconductors and the projected superconducting state of liquid metallic hydrogen.

ACKNOWLEDGMENTS

It is my pleasure to thank Egor Babaev and Alexander Mel'nikov for stimulating discussions. I am grateful for hospitality to the Department of Theoretical Physics at The Royal Institute of Technology where the final part of the work was done. This work was supported by Swedish Research Council, "Dynasty" Foundation, Presidential RSS Council (Grant No. MK- 4211.2011.2), Russian Foundation for Basic Research, by Programs of RAS "Quantum Physics of Condensed Matter" and "Strongly correlated electrons in semiconductors, metals, superconductors and magnetic materials", and by Russian Ministry of education under the Federal program "Scientific and educational personnel of innovative Russia".

APPENDIX : DERIVATION OF THE INTEGRAL EQUATION (26)

(i) To find the energy $F_m(x_v)$ let us consider at first the interaction of the probe vortex with the vortex positioned at the coordinate $\mathbf{r} = (x, y)$ and the antivortex at the coordinate $\tilde{\mathbf{r}} = (-x, y)$. Applying Eq. (7) we take into account only the energy of the interaction between vortices and obtain

$$F_m(\mathbf{r_v}, \mathbf{r}) = 2\left(\frac{\phi_A}{4\pi\lambda}\right)^2 \left[K_0\left(\frac{|\mathbf{r}-\mathbf{r_v}|}{\lambda}\right) - K_0\left(\frac{|\tilde{\mathbf{r}}-\mathbf{r_v}|}{\lambda}\right)\right]. \tag{A1}$$

Now, to find the total energy $F_m(x_v)$, we integrate over the positions of all vortices to obtain

$$F_m(x_v) = \int_{-\infty}^{\infty} dy \int_0^{\infty} dx\, n(x) F_m(\mathbf{r_v}, \mathbf{r}). \tag{A2}$$

To perform the integration in Eq. (A2), we use the following relation,

$$\int_{-\infty}^{\infty} K_0\left(\sqrt{x^2+y^2}\right) dy = \pi e^{-|x|},$$

and obtain

$$F_m(x_v) = \frac{\phi_A^2}{8\lambda\pi}\int_0^\infty \left[\exp\left(-\frac{|x-x_v|}{\lambda}\right) - \exp\left(-\frac{|x+x_v|}{\lambda}\right)\right] n(x)dx. \quad \text{(A3)}$$

(ii) According to Eq. (6), energy $F_{nc}(x_v)$ is determined by the following expression,

$$F_{nc}(x_v) = \frac{1}{\pi}\frac{\phi_A\phi_B}{(4\pi\lambda)^2}\int d^2\mathbf{r}\nabla\varphi\nabla\varphi_v, \quad \text{(A4)}$$

where

$$\varphi_v = \arctan\left(\frac{y-y_v}{x-x_v}\right)$$

is the phase distribution created by the probe vortex and

$$\varphi_v = \sum_i m_i \arctan\left(\frac{y-y_i}{x-x_i}\right)$$

is the phase created by all other vortices ($m_i = 1$) and antivortices ($m_i = -1$). To evaluate expression (A4) let us consider again the interaction of the probe vortex with the vortex positioned at the coordinate $\mathbf{r} = (x,y)$ and the antivortex at the coordinate $\tilde{\mathbf{r}} = (-x,y)$. Then we have that

$$F_{nc}(\mathbf{r_v},\mathbf{r}) = 2\frac{\phi_A\phi_B}{(4\pi\lambda)^2}\ln\left(\frac{|\mathbf{r}+\mathbf{r_v}|}{|\mathbf{r}-\mathbf{r_v}|}\right).$$

This expression is divergent at the point $\mathbf{r} = \mathbf{r_v}$, which should be cut off at the vortex core size ξ_A. However, this singularity is integrable and we do not introduce this cutoff here. Then we should sum the contributions from all vortices according to the expression

$$F_{nc}(x_v) = \int_{-\infty}^{\infty} dy \int_0^\infty dx\, n(x) F_{nc}(\mathbf{r_v},\mathbf{r}). \quad \text{(A5)}$$

The integration over the coordinate y in Eq. (A5) can be performed using the relation

$$\int_{-\infty}^{\infty}\ln\left(\frac{|\mathbf{r}+\mathbf{r_v}|}{|\mathbf{r}-\mathbf{r_v}|}\right)dy = \begin{cases} 2\pi x_v & \text{for} \quad x > x_v, \\ 2\pi x & \text{for} \quad x < x_v. \end{cases}$$

Then we obtain

$$F_{nc}(x_v) = \frac{\phi_A\phi_B}{4\pi\lambda^2}\left[\int_0^{x_v} x n(x)dx + \int_{x_v}^\infty x_v n(x)dx\right]. \quad \text{(A6)}$$

(iii) Finally the energy $W(x_v)$ determining the interaction of the probe vortex with external magnetic field can be found from Eqs. (14) and (15):

$$W(x_v) = -\frac{\phi_A}{4\pi}H_0(1-e^{-x_v/\lambda}). \quad \text{(A7)}$$

Summing all the contributions to the Gibbs energy (A3), (A6), and (A7), we obtain the total force acting on a probe vortex:

$$\mathbf{f} = \frac{\partial}{\partial\mathbf{r_v}}F_G = (f_m + f_{nc} + f_{\text{ext}})\mathbf{x_0},$$

where

$$f_m(x_v) = \frac{\phi_A^2}{8\pi\lambda^2}\int_0^\infty \left[\frac{(x-x_v)}{|x-x_v|}\exp\left(-\frac{|x+x_v|}{\lambda}\right) + \exp\left(-\frac{|x+x_v|}{\lambda}\right)\right] n(x)dx, \quad \text{(A8)}$$

$$f_{nc} = \frac{\phi_A\phi_B}{4\pi\lambda^2}\int_{x_v}^\infty n(x)dx, \quad \text{(A9)}$$

and

$$f_{\text{ext}} = -\frac{\phi_A}{4\pi\lambda}H_0 e^{-x_v/\lambda}. \quad \text{(A10)}$$

The condition of the probe vortex stationarity $\mathbf{f} = 0$ yields the integral Eq. (26), where the coordinates x and x_v are normalized to the length scale λ.

[1] T. Muranaka *et al.*, in *Frontiers in Superconducting Materials*, edited by A. V. Narlikar (Springer, Berlin, 2005).

[2] V. Barzykin, L. P. Gor'kov, JETP Lett. **88**, 142 (2008); S. Raghu, Xiao-Liang Qi, Chao-Xing Liu, D. J. Scalapino, and Shou-Cheng Zhang, Phys. Rev. B **77**, 220503 (2008).

[3] M. Jourdan, A. Zakharov, M. Foerster, and H. Adrian, Phys. Rev. Lett. **93**, 097001 (2004); G. Seyfarth, J. P. Brison, M.-A. Measson, J. Flouquet, K. Izawa, Y. Matsuda, H. Sugawara, and H. Sato, *ibid.* **95**, 107004 (2005).

[4] S. V. Shulga, S.-L. Drechsler, G. Fuchs, K.-H. Muller, K. Winzer, M. Heinecke, and K. Krug, Phys. Rev. Lett. **80**, 1730 (1998).

[5] M. I. Eremets, I. A. Trojan, S. A. Medvedev, J. S. Tse, Y. Yao, Science **319**, 1506 (2008); S. Deemyad and I. F. Silvera, Phys. Rev. Lett. **100**, 155701 (2008).

[6] N. W. Ashcroft, J. Phys. Condens. Matter **12**, A129 (2000); Phys. Rev. Lett. **92**, 187002 (2004); K. Moulopoulos and N. W. Ashcroft, *ibid.* **66**, 2915 (1991).

[7] E. Babaev, A. Sudbø, and N. W. Ashcroft, Nature (London) **431**, 666 (2004).

[8] E. Babaev, A. Sudbø and N. W. Ashcroft, Phys. Rev. Lett. **95**, 105301 (2005).

[9] V. A. Moskalenko, Phys. Met. Metallogr. **8**, 503 (1959).

[10] H. Suhl, B. T. Matthias, and L. R. Walker, Phys. Rev. Lett. **3**, 552 (1959).

[11] E. Babaev and N. W. Ashcroft, Nat. Phys. **3**, 530 (2007).

[12] E. Babaev and M. Speight, Phys. Rev. B **72**, 180502 (2005).

[13] V. Moshchalkov, M. Menghini, T. Nishio, Q. H. Chen, A. V. Silhanek, V. H. Dao, L. F. Chibotaru, N. D. Zhigadlo, and J. Karpinski, Phys. Rev. Lett. **102**, 117001 (2009).

[14] E. Babaev, Phys. Rev. Lett. **89**, 067001 (2002).

[15] M. M. Salomaa and G. E. Volovik, Rev. Mod. Phys. **59**, 533 (1987).

[16] R. Barnett, A. Turner, and E. Demler, Phys. Rev. A **76**, 013605 (2007).

[17] A. J. Berlinsky, A. L. Fetter, M. Franz, C. Kallin, and P. I. Soininen, Phys. Rev. Lett. **75**, 2200 (1995); M. Franz, C. Kallin, P. I. Soininen, A. J. Berlinsky, and A. L. Fetter, Phys. Rev. B **53**, 5795 (1996); A. S. Melnikov, I. M. Nefedov, D. A. Ryzhov, I. A. Shereshevskii, and P. P. Vysheslavtsev, *ibid.* **62**, 11820 (2000).

[18] E. Smorgrav, J. Smiseth, E. Babaev, and A. Sudbø, Phys. Rev. Lett. **94**, 096401 (2005).

[19] J. Goryo, S. Soma, and H. Matsukawa, Europhys. Lett. **80**, 17002 (2007).

[20]E. Babaev, Nucl. Phys. B **686**, 397 (2004).
[21]L. F. Chibotaru, V. H. Dao, and A. Ceulemans, Europhys. Lett. **78**, 47001 (2007).
[22]R. Geurts, M. V. Milosevic, and F. M. Peeters, Phys. Rev. B **81**, 214514 (2010).
[23]P. B. Jones, Mon. Not. R. Astron. Soc. **371**, 1327 (2006).
[24]E. Babaev, Phys. Rev. Lett. **103**, 231101 (2009).
[25]C. P. Bean and J. D. Livingston, Phys. Rev. Lett. **12**, 14 (1964).
[26]V. V. Schmidt and G. S. Mkrtchyan, Sov. Phys. Usp. **17**, 170 (1974).
[27]C. Iniotakis, T. Dahm, and N. Schopohl, Phys. Rev. Lett. **100**, 037002 (2008); A. Zare, T. Dahm, and N. Schopohl, *ibid*. **104**, 237001 (2010).
[28]E. Babaev, J. Jäykkä, and M. Speight, Phys. Rev. Lett. **103**, 237002 (2009).
[29]*Handbook of Mathematical Functions with Formulas, Graphs, and Mathematical Tables*, edited by M. Abramowitz and I. A. Stegun (Dover, New York, 1972).
[30]P. G. de Gennes, *Superconductivity of Metals and Alloys* (Benjamin, New York, 1966).
[31]Y. Y. Goldschmidt and S. Tyagi, Phys. Rev. B **71**, 014503 (2005).